Hepatitis Delta Virus Ribozymes Fold To Generate a Solvent-Inaccessible Core with Essential Nucleotides Near the Cleavage Site Phosphate†

Sarah P. Rosenstein and Michael D. Been*

Department of Biochemistry, Box 3711, Duke University Medical Center, Durham, North Carolina 27710

Received April 25, 1996; Revised Manuscript Received July 8, 1996⊗

ABSTRACT: Self-cleaving sequences or ribozymes from the hepatitis delta virus (HDV) genomic RNA and its complement form similar secondary structures that suggest a core region and potential active site composed of "single-stranded" sequences. However, there is little data on tertiary interactions in these ribozymes, therefore structural features were investigated using cross-linking and hydroxyl radical cleavage. Cross-links in *cis* and *trans* forms of the antigenomic RNA were generated using the photoactivatable azidophenacyl group tethered to the cleavage site phosphate. Specific cross-links formed to J4/2, and to the 3′ sides of P3 and L3. Different sites were cross-linked in low salt or monovalent cations versus divalent cations, suggesting a metal ion-dependent conformational change near the cleavage site. The solvent-inaccessible regions of both the genomic and antigenomic ribozymes were revealed by cleavage in Fe(II)−EDTA. In Mg^{2+}, backbone segments most strongly protected from solvent-based hydroxyl radicals were mapped to J4/2 and parts of L3. Similar patterns of protection were seen in *trans*-acting ribozymes bound to a product oligonucleotide. These data provide evidence for a common tertiary structure for the HDV ribozymes. They would be consistent with a model in which the end of P1, including the cleavage site phosphate and the nucleotide 5′ to the cleavage site, is positioned in an active site pocket or cleft formed by the three single-stranded regions, L3, J4/2, and J1/4.

Genomic and antigenomic RNAs of hepatitis delta virus (HDV)[1] contain self-cleaving sequences (ribozymes) that appear to be responsible for processing of linear multimeric RNA products generated during rolling circle replication of the RNA to monomer sequences (Jeng et al., 1996; Kuo et al., 1988; MacNaughton et al., 1993; Sharmeen et al., 1988; Wu et al., 1989). The HDV ribozymes require only Mg^{2+} or Ca^{2+} for optimal catalytic activity in vitro (Kuo et al., 1988; Sharmeen et al., 1988; Wu et al., 1989). A direct role of metal ions in catalysis has not yet been demonstrated; however, there is good evidence that divalent cation is required to stabilize the folded form of the RNA in solution (Rosenstein & Been, 1991). Cleavage is thought to proceed via a transesterification reaction since the products of the reaction are a 5′ fragment with a 2′,3′-cyclic phosphate and a 3′ fragment with a 5′ hydroxyl group (Kuo et al., 1988; Sharmeen et al., 1988; Wu et al., 1989). Consistent with the proposed mechanism, the adjacent 2′ hydroxyl group is required for cleavage (Perrotta & Been, 1992). The minimum sequence required for self-cleavage of the genomic (Perrotta & Been, 1990) and antigenomic ribozymes (Perrotta & Been, 1990) can be folded into similar structures containing four stems, or paired sequences, designated P1−P4 (Been, 1994; Perrotta & Been, 1991; Rosenstein & Been, 1991) (Figure 1A and B). These structures are consistent with site-directed mutagenesis (Been et al., 1992; Perrotta & Been, 1991, 1993; Thill et al., 1993), ribonuclease probing (Rosenstein & Been, 1991), and chemical modification studies (Belinsky et al., 1993; Kumar et al., 1994; Wu et al., 1992).

Reconstitution of active ribozymes from fragments of the self-cleaving sequence has been accomplished in two ways (Branch & Robertson, 1991; Perrotta & Been, 1992). Scission of the antigenomic RNA in J1/2 produced a ribozyme missing only the 5′ side of P1; the 3′ side of P1 in this ribozyme pairs with the substrate to form P1 and is capable of catalyzing cleavage of the substrate RNA (Perrotta & Been, 1992) (Figure 1C and D). Similar variations of this form include a *trans*-acting ribozyme generated with genomic RNA (Thill et al., 1993) and a *trans*-acting ribozyme designed as a composite of both genomic and antigenomic sequences (Been et al., 1992). The sequence specificity of the reaction can be altered by changes to the ribozyme portion of P1 (Branch & Robertson, 1991; Perrotta & Been, 1992). Alternatively, the ribozyme can be separated at the end of P4, generating a substrate that contains P1, P3/L3, J1/4, and the 5′ sides of P2 and P4 and a ribozyme that contains the 3′ sides of P4 and P2 together with J4/2 (Branch & Robertson, 1991; Wu et al., 1992). This mode of fragmentation, originally interpreted in terms of a different secondary structure, is also consistent with the pseudoknot secondary structure (Perrotta & Been, 1993).

Although the secondary structure is now well established, it alone does not define features of the overall structure which form an active site. The question of how the HDV RNA folds to bring essential nucleotides necessary for catalysis together and in close proximity to the cleavage site requires further information about the tertiary structure. Mutagenesis of single-stranded regions has been used to help define essential residues in the ribozymes (Kumar et al., 1992; Perrotta & Been, 1996; Tanner et al., 1994; Wu & Huang, 1992; Wu et al., 1993). These data suggest that sequences in L3, J1/4, and J4/2 are important for cleavage activity and

† This work was supported by grants from the NIH (GM40689 and GM47233).

⊗ Abstract published in *Advance ACS Abstracts,* August 15, 1996.

[1] Abbreviations: HDV, hepatitis delta virus; GMPS, guanosine monophosphorothioate; AzBr, *p*-azidophenacyl bromide; Az-RNA, azidophenylated RNA; L, loop; J, joining region.

S0006-2960(96)00998-1 CCC: $12.00

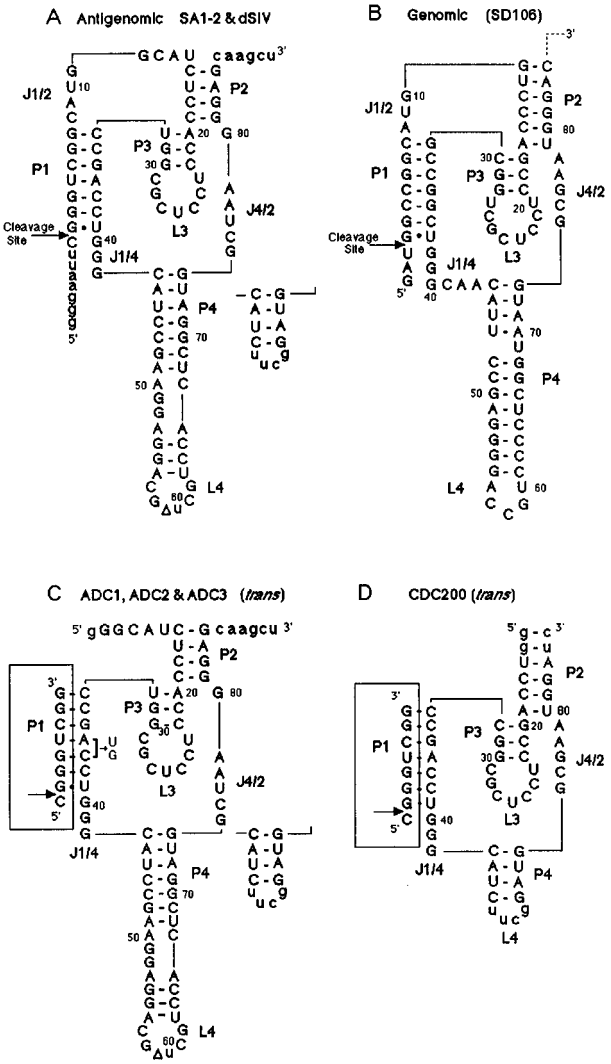

FIGURE 1: Secondary structures of HDV ribozymes. (A) Antigenomic SA1-2 and dSIV. Uppercase letters are the HDV sequence, lowercase letters are the vector-derived or modified sequence (L4). The arrow indicates the site of cleavage. Paired sequences (P1−P4) are numbered 5′ to 3′ from the cleavage site. Loops (L) and joining regions (J) are labeled relative to the pairings. Nucleotide numbering is from the cleavage site. The complete sequence of SA1-2 and the shortened P4 of dSIV are shown. Numbering of the core sequences in dSIV is the same as for SA1-2. For SA1-2P and dSIVP RNAs, transcription initiates at G1 (cleavage site arrow). (B) Genomic SD106 ribozyme. (C) Antigenomic *trans*-acting ribozymes and substrate (box) sequence. The complete sequence for ribozyme ADC1 is shown. ADC2 is essentially ADC1 with two nucleotide changes on the 3′ side of P1 indicated by the bracket. ADC3 is a derivative of ADC1 in which P4 is shortened (right). (D) Composite *trans*-acting ribozyme CDC200 and substrate (box). Nucleotide numbering of core nucleotides is the same as SA1-2.

are thus consistent with the fragmentation and deletion studies which demonstrated that J1/2 and most of P4/L4 are not required (Been et al., 1992; Branch & Robertson, 1991; Perrotta & Been, 1992; Wu et al., 1992). Tanner et al. (1994) have modeled a three-dimensional structure of the genomic sequence which incorporates established features of the secondary structure and information obtained from mutagenesis of bases in the single-stranded regions. This model places several of the key residues close to the cleavage site phosphate. However, with the exception of a homopurine base pair identified at the base of P4 (Been & Perrotta, 1995), extensive mutagenesis has not provided any information about potential interactions within the core. In addition, there is little additional evidence pertaining to the overall tertiary folding of these RNAs which could provide clues to the structure and thus help evaluate and refine that model. It is difficult with the currently available information to be confident either about the orientation of the helices relative to each other or about details of structures within and between the "single-stranded" regions J1/4, J4/2, and L3.

Secondary structure similarities between the genomic and antigenomic HDV ribozyme sequences imply that their tertiary structures should also be related, therefore data obtained with either HDV ribozyme could contribute to the understanding of both structures. Biochemical methods that have revealed tertiary information in other ribozymes include hydroxyl radical cleavage (Celander & Cech, 1990; Latham & Cech, 1989) and photo-induced cross-linking (Burgin & Pace, 1990; Nolan et al., 1993; Wang et al., 1993). In a solvent-dependent reaction, Fe(II)−EDTA generates hydroxyl radicals that cleave the phosphoribose backbone near the site of their formation (Burkhoff & Tullius, 1987; Hertzberg & Dervan, 1984). A photoactivatable cross-linking reagent, azidophenacyl bromide, has been coupled to tRNA and used successfully to identify regions of RNase P RNA in close proximity to the tRNA in binary complexes (Burgin & Pace, 1990). This method has been also been applied to the *Tetrahymena* group I intron (Wang et al., 1993). We report here that the cross-linking approach identified sequences within the antigenomic RNA that specifically cross-link to the cleavage site phosphate. Several of these nucleotides are in or near regions which were determined to be inaccessible to solvent in the Fe(II)−EDTA cleavage experiments. This information provides important constraints for models of the tertiary structure of the HDV self-cleaving RNA sequences and defines sequences that are likely to form the catalytic center.

EXPERIMENTAL PROCEDURES

Enzymes, Reagents, and Chemicals. T7 RNA polymerase was purified from an over-expressing clone (Davanloo et al., 1984). Gifts of guanosine 5′ monophosphorothioate (GMPS) were kindly provided by F. Eckstein (Max Planck Institute, Göttingen) and J. Nolan and N. Pace (Indiana University). *p*-Azidophenacyl bromide (AzBr) was purchased from Sigma, hydrogen peroxide from Mallinckrodt, ammonium iron (III) hexahydrate and L-ascorbate from Aldrich, and dithiothreitol (DTT) and ^{32}P-labeled nucleotides from ICN. All other reagents, restriction endonucleases, nucleotides, and enzymes were purchased from various commercial sources.

Plasmids. The plasmids pSA1-2P and pdSIVP were generated by oligonucleotide-directed deletion mutagenesis using a uracil-containing single-stranded form of the plasmids pSA1-2 and pdSIV (Been et al., 1992; Perrotta & Been, 1991). Both are derivatives of the antigenomic ribozyme sequence but are designed such that transcription starts precisely at the cleavage site to generate a sequence identical to 3′ product RNA except that it contains phosphate(s) at the 5′ end. Deletions were identified by sequencing and plasmid DNA was purified by CsCl equilibrium density centrifugation in the presence of ethidium bromide (Maniatis et al., 1982). The other plasmids used in this study, pADC1, pADC2, pADC3, pCDC200, and pSD106, have been described elsewhere (Been et al., 1992; Perrotta & Been, 1990).

Preparation of Photoagent-Containing RNA. RNA for interstrand cross-linking studies was prepared by in vitro

transcription of the *Hin*dIII-linearized pSA1-2P and pdSIVP DNA in the presence of guanosine 5′ monophosphorothioate (GMPS). Transcription reactions contained: 50 μg of linear plasmid DNA/mL, 40 mM Tris-HCl (pH 7.5), 20 mM $MgCl_2$, 9 mM DTT, 2 mM spermidine, 0.1 mg of T7 RNA polymerase/mL, 4 mM GMPS, and 0.2 mM each of the ribonucleoside triphosphates (rNTPs) (Burgin & Pace, 1990). Incubation was for 2 h at 37 °C, and the RNA was gel purified and eluted into 10 mM Tris (pH 7.5), 1 mM EDTA, 0.1% sodium dodecyl sulfate (SDS), and 1 mM DTT overnight at 4 °C. A portion of the RNA (20 pmol) was then 3′ end-labeled with [^{32}P]pCp (Perrotta & Been, 1990) and gel purified. The 3′ end-labeled RNA was coupled with azidophenacyl bromide essentially as described by Burgin and Pace (1990) and Wang et al. (1993). ^{32}P-labeled RNA (0.25−0.35 μCi) was incubated at room temperature in the dark for 1 h in 20 mM sodium bicarbonate (pH 9.0) and 40% methanol containing 5−50 mM AzBr. RNA for control experiments was similarly treated but without the AzBr. An equal volume of 10 mM Tris (pH 7.5)/1 mM EDTA was then added, and excess AzBr was removed by extracting two times with an equal volume of buffered phenol. The photoagent-containing RNA (Az-RNA) was recovered by ethanol precipitation, resuspended in 0.1 mM EDTA, and kept in the dark in amber Eppendorf tubes (United Laboratory Plastics) covered with aluminum foil. In a set of parallel reactions using a self-cleaving form of the RNA, for which modification was easier to quantify, 80% of the total RNA was estimated to be modified when it was GMPS-primed and treated with AzBr (S.P.R., unpublished data).

GMPS-containing oligonucleotide for intrastrand cross-linking to a *trans*-active ribozyme was prepared by omitting ATP from the transcription reaction. In the absence of ATP, a short product accumulates when the polymerase encounters the first T in the template. Transcription products were purified on a 20% polyacrylamide gel; the oligonucleotide that migrated to the same position as a labeled 8mer marker was located by autoradiography, excised from the gel and eluted at 4 °C. The sequence was confirmed by end-labeling and enzymatic sequencing (Rosenstein & Been, 1991). The 8mer was reacted with AzBr and purified as described above.

trans-Acting ribozymes were prepared by in vitro transcription of *Hin*dIII-linearized pADC1 and pADC3 DNA and purified by gel electrophoresis. Ribozyme RNA was dephosphorylated with calf intestinal phosphatase and labeled at the 5′ end with ^{32}P (Perrotta & Been, 1990).

Intramolecular Cross-Links. The 3′ end-labeled precursor-analog Az-RNA (or control RNA not coupled) was heated to 90 °C for 2 min in water or 10 M formamide. Then one-tenth volume of the sample buffer was added, and the sample was immediately shifted to a 37 °C water bath for 10 min. The final concentrations after addition of sample buffer were 40 mM Tris-HCl (pH 8.0), 1 mM EDTA, alone or with 11 mM $MgCl_2$, 11 mM $CaCl_2$, or 100 mM NaCl. Following the 10 min incubation, 5 μL of the RNA solution was kept at room temperature in the dark, while another 5 μL was spotted onto plastic wrap covering an aluminum block that was equilibrated in water at room temperature. This sample was covered with a Petri dish to filter out light <300 nm (Burgin & Pace, 1990) and irradiated for 10 min with UV light (model FBUVM80 312 nm lamp, Fisher Biotech) held directly above the Petri dish at a distance of 2−3 cm. All samples were recovered into an equal volume of 95% formamide containing 50 mM EDTA and 2 mM DTT, heated to 95 °C for 3 min, and fractionated on a 15% polyacrylamide gel containing 50% w/v urea. The gel was visualized by autoradiography and quantified using a phosphorimager.

DTT was added to the loading buffer to reduce RNA complex formation which occurred only with GMPS-containing RNA. These presumptive dimer species migrated in a position just below that of the intramolecular cross-linked species in the gel. These dimers were most likely formed after the GMPS-containing RNA was recovered from the DTT-containing gel elution buffer, but disappeared when DTT was included in the loading buffer. The percent of RNA that was in a cross-linked adduct was not changed by the presence of DTT in the loading buffer (data not shown).

To determine the location of the cross-links, the cross-linking reaction was scaled up to 70 μL (0.5 μCi of labeled RNA), UV irradiated in 10 μL aliquots, recovered into loading buffer, and run on a gel. Cross-linked bands were visualized by autoradiography, excised, and eluted at 4 °C in 10 mM Tris (pH 7.5), 1 mM EDTA, and 0.1% SDS. Partial alkaline hydrolysis of the RNA was as described previously (Rosenstein & Been, 1991). Sequencing markers were generated by treatment with RNase T1 and U2 (Rosenstein & Been, 1991). Samples were fractionated by electrophoresis on a 15% polyacrylamide sequencing gel, and the results were visualized by autoradiography.

Intermolecular Cross-Links. Uniformly labeled 5′ Az-8mer substrate analog (1 nM) was incubated with ribozyme ADC1, ADC2, or ADC3 (20 nM) at 37 °C for 10−15 min in the same buffers used for intramolecular cross-linking and was then shifted to room temperature and irradiated as described above. Separation and visualization of cross-linked species were as described above except DTT was not included in the loading buffer. Large-scale preparations of cross-linked species and determination of cross-link positions were done using similar amounts of ribozyme and analog in a larger volume as described above.

Fe(II)−EDTA Cleavage Analysis. RNA was transcribed from *Eco*RI-linearized pSD106 and *Hin*dIII-linearized pdSIV, pSA1-2, pADC1, pADC2, pADC3, and pCDC200 as described above. For the self-cleaving constructs (pSD106, pSA1-2 and pdSIV), only the 3′ cleavage product RNA was isolated. *trans*-Acting ribozymes were 5′ end-labeled after dephosphorylation (Been et al., 1992) and cleavage product RNAs were 5′ end-labeled directly (Rosenstein & Been, 1991).

Hydroxyl radical cleavage of the end-labeled RNA was carried out using one of two protocols: the hydrogen peroxide method described by Burkoff and Tullius (1987) and the molecular oxygen method described by Latham and Cech (1989). Both methods gave identical results. For the peroxide method, 0.1−0.15 μCi of 5′ end-labeled RNA (SD106, SA1-2, or dSIV) was heated at 90 °C for 2 min in 0.1 mM EDTA. Next one-quarter volume of buffer was immediately added, and the sample was incubated at room temperature for 2 min. The final concentrations in a 10 μL reaction were 35 mM Tris (pH 7.5) and 10 mM $MgCl_2$. One-tenth volumes each of 10 mM ammonium iron (II) sulfate/20 mM EDTA (pH 8.0), 100 mM sodium ascorbate, and 0.6% hydrogen peroxide were added in that order to the sample, and the reaction was allowed to proceed for 2.5 min at room temperature in the dark. Following this, an equal volume of 95% formamide/50 mM EDTA/0.025% each of XC and BPB was added, and the samples were heated to 95 °C and loaded on a 6%−15% polyacrylamide (29:1 acryla-

mide:bisacrylamide) sequencing gel containing 8.3 M urea. Reactions using the molecular oxygen method were similar, except that 50 mM DTT was added instead of ascorbate and peroxide, and the reaction was incubated for 90 min at 42 °C. Reactions with the *trans*-acting RNA using the hydrogen peroxide method were identical to those for *cis*-acting RNA except that 5′ end-labeled ribozyme (ADC1, ADC2, ADC3, or CDC200) and product oligonucleotide, DHP9 (5′-GGGUCGG-3′), were pre-incubated at 37 °C for 10−15 min in buffer (instead of heating to 90 °C) . The results were visualized by autoradiography and quantified using a phosphorimager.

RESULTS

Intramolecular Cross-Linking of RNA to the Active Site Phosphate (cis Ribozyme). In the HDV ribozyme, a single nucleotide 5′ to the cleavage site is sufficient for cleavage and there is little base preference at that position (Perrotta & Been, 1990, 1992). In pSA1-2P and pdSIVP DNA, transcription from the T7 promoter initiated at G1, the nucleotide immediately 3′ to the cleavage site. In the presence of guanosine 5′ monophosphorothioate (GMPS), transcription yields RNA with a 5′ thiophosphate. Using *p*-azidophenacyl bromide, the azidophenacyl group was coupled to the sulfur via a nucleophilic displacement reaction as described by Burgin and Pace (1990). Therefore, a noncleavable precursor analog is produced in which the nucleotide 5′ of the cleavage site is replaced with the cross-linking agent.

5′ Az-SA1-2P or Az-dSIVP RNA radiolabeled with ^{32}P at the 3′ end was pre-incubated at 37 °C in the presence of 10 mM Mg^{2+} at pH 8.0, shifted to 24 °C and irradiated with 312 nm light to promote cross-linking. The azidophenacyl group is specifically activated by UV light to form a highly reactive nitrene which can insert into nearby bonds (Burgin & Pace, 1990). An intramolecular cross-link would be expected to generate a loop, the size of which would be dependent on the location of the cross-link. Upon fractionation by polyacrylamide gel electrophoresis under denaturing conditions, the Az-RNA that was irradiated with UV light produced a fairly discrete, slower migrating species (Figure 2A, lanes 7, 8, 15, and 16). Because a loop may alter mobility, the slower migrating species were thought to contain a UV-inducible cross-link. Omitting either the coupling step or the UV light treatment resulted in loss of the slower migrating species (Figure 2A, lanes 1−6 and 9−14). In addition, RNA that was primed with GMP instead of GMPS did not form the slower migrating species (data not shown). These controls confirm that the presumed cross-linked species were formed only when the RNA was azidophenylacylated and treated with UV light. There was no change in the percent cross-linked species for either RNA species when the RNA concentration was varied over a 500-fold range (16 pM to 8.1 nM; data not shown).

The mobility of the cross-linked species was observed to vary with metal ion used; RNA incubated in Mg^{2+} and then irradiated resulted in a product that migrated slightly faster than RNA incubated without divalent cation. This metal ion effect on mobility and presumably location of the cross-link was seen for both SA1-2P and dSIVP (compare lanes 7 and 8 and lanes 15 and 16 in Figure 2A). The extent of cross-linking ranged from 3% to 5% in the experiment shown. The effect of incubation conditions on mobility (and presumably the cross-link position) was investigated to see if this correlated with reaction conditions. HDV ribozymes self-cleave in the presence of a variety of divalent cations but are most active in Mg^{2+} and Ca^{2+} (Wu et al., 1989); there is little or no activity in the presence of monovalent salt alone. With most versions of the wild-type HDV ribozyme sequence, moderate to high levels of denaturants (e.g., 5−9 M urea, 10−18 M formamide) either increase the rate of cleavage (Rosenstein & Been, 1990) or have little or no effect. To correlate formation of the faster migrating cross-linked species with conditions which support self-cleavage, cross-link formation in 10 mM Ca^{2+} or in 10 mM Mg^{2+} plus 10 M formamide was compared to cross-linking in 100 mM Na^{+}. After irradiation with 312 nm light, Az-dSIVP RNA formed cross-linked species in all five conditions tested (Figure 2B, lanes 6−10). In Tris/EDTA alone or with 100 mM Na^{+}, the slower migrating product was again seen (compare lanes 6 and 7 in Figure 2B). In the presence of 10 mM Ca^{2+}, 10 mM Mg^{2+}, or 10 mM Mg^{2+} plus 40% formamide, the faster migrating product formed (compare lanes 8−10 in Figure 2B). No cross-linked species were seen in the absence of UV light (Figure 2B, lanes 1−5). The same results were obtained when 5′ Az-SA1-2P RNA was used (data not shown).

To map the locations of the cross-links, the slow-migrating RNA was isolated from a preparative gel and a ladder of fragments was generated by partial alkaline cleavage. Cleavage between the labeled 3′ end and the cross-link should generate a ladder of small labeled fragments differing in size by a single nucleotide. Cleavage of the RNA in the looped region will generate a Y or branched species with one branch still labeled. This branched species would be expected to continue to migrate slowly in the gel. Partial hydrolysis of the cross-linked species gave a ladder of fragments only near the bottom of the gel (Figure 2C, lanes 4, 5, 9, and 10). RNA that did not shift in mobility when treated with UV light was also isolated and treated with alkali; it generated a complete ladder with no apparent anomalies (data not shown).

The positions of the cross-links were identified by comparison to sequencing ladders of unmodified RNA (Figure 2C, lanes 1−3, 6−8). For reasons that are not entirely clear, we find that the 3′ end of RNA isolated from transcriptions primed with GMPS or GMP is more heterogeneous than RNA made with only nucleoside triphosphates (data not shown); therefore, sequencing markers of RNA synthesized with only nucleoside triphosphates were used to help map the cross-link. An alignment of alkaline ladder bands in the modified (Figure 2C, lanes 4, 5, 9, and 10) and unmodified samples (lane 3) revealed the location of cross-links to be near the 3′ end of the ribozyme, in J4/2. With both SA1-2P RNA and dSIVP RNA cross-linked in the absence of Mg^{2+} (Tris/EDTA alone), a ladder of fragments was seen from the bottom of the gel to a position comigrating with a band resulting from an RNase U2 cut between A78 and A79 (arrow pointing to A78, lanes 1 and 6). A very faint band could be seen in the cross-linked RNA above that position, but little was seen above that (lanes 4 and 9). Because the RNA was 3′ end-labeled, an RNase U2 fragment resulting from cutting between A78 and A79 would contain sequence from the 3′ end through A79. The significant decrease in the intensity of the hydrolyzed bands after this point suggested that the cross-link was to A78 (Figure 3A). Also, the faint band corresponding to one nucleotide above

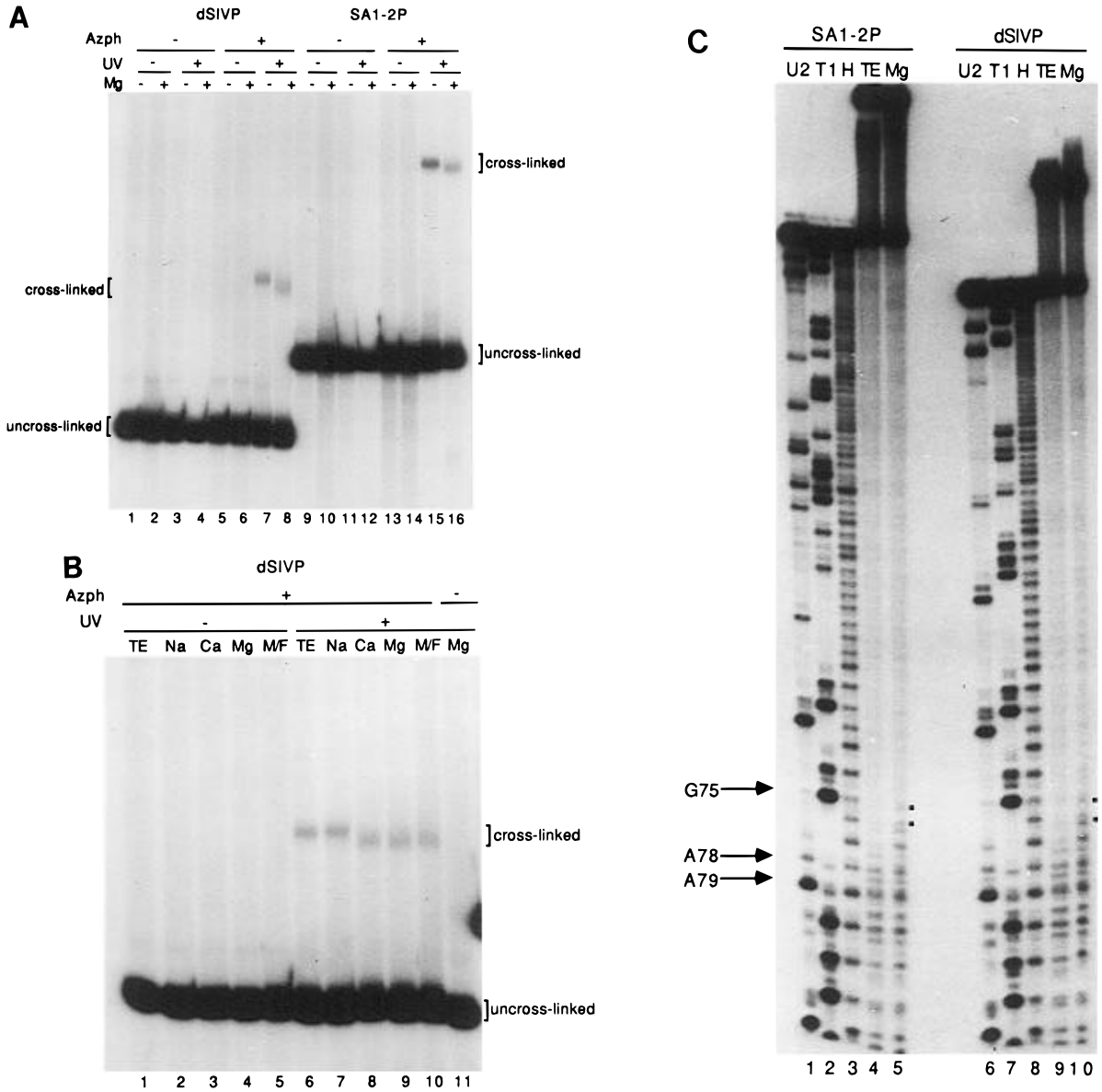

FIGURE 2: Intramolecular cross-linking of ribozymes. (A) Cross-linking of dSIVP and SA1-2P Az-RNA. The 3′ end-labeled GMPS-primed RNA derivatized with azidophenacyl bromide (+Azph) was UV irradiated at 312 nm (+UV) in the absence or presence of $MgCl_2$ (±Mg) (lanes 7 and 8 and lanes 15 and 16). Samples were run on a 15% polyacrylamide gel containing 50% urea, and an autoradiograph of the gel is shown. Controls in which either the azidophenacyl group, the UV treatment, or both are omitted are also shown. (B) The altered mobility of cross-linked dSIVP RNA correlates with the presence of divalent cation. Labeled Az-RNA was irradiated in the presence of Tris/EDTA alone (TE; lanes 1 and 6) or with 100 mM NaCl (Na; lanes 2 and 7), 11 mM $CaCl_2$ (Ca; lanes 3 and 8), 11 mM $MgCl_2$ (Mg; lanes 4, 9, and 11) or 11 mM $MgCl_2$ with 40% formamide (Mg/F; lanes 5 and 10). Samples were analyzed as described for A. (C) Mapping the position of cross-links in dSIVP and SA1-2P RNA. Gel purified cross-linked species generated in the presence of Tris/EDTA alone (lanes 4 and 9) or with Mg^{2+} (lanes 5 and 10) were partially hydrolyzed with alkali and analyzed on a sequencing gel. The 3′ end-labeled GTP-primed RNA from standard *in vitro* transcriptions of plasmids pSA1-2P or pdSIVP was used to generate an A ladder (U2; lanes 1 and 6), a G ladder (T1; lanes 2 and 7), and an alkaline hydrolysis ladder (H; lanes 3 and 8). Dots are used to indicate the positions of bands corresponding to positions of the light bands at C76 and G75.

this would indicate a cross-link to U77, although to a lesser amount. In the presence of Mg^{2+}, the intensity of the bands in the hydrolysis ladder from the cross-linked species was similar to the control lane up to position U77 (compare lanes 3 and 5 and lanes 8 and 10). Above this, two bands of lesser intensity, but of similar intensity to each other, were observed (lanes 5 and 10). This was interpreted to mean that, in the presence of 10 mM Mg^{2+}, the cleavage site phosphate was cross-linked to C76 and G75 at about the same frequency (Figure 3A).

Cross-Linking of RNA to the Active Site Phosphate in trans. The HDV self-cleaving sequence can be separated into an "enzyme" and a "substrate" that can annealed to form an active ribozyme. To detect cross-linking in the complex, the *trans*-acting ribozymes ADC1, ADC2, and ADC3 (Figure 1C) (Been et al., 1992; Perrotta & Been, 1992) were 5′ end-labeled. A product analog RNA (nt +1 to +8, relative to the cleavage site) with GMPS at the 5′ end was prepared as described in experimental procedures and reacted with azidophenacyl bromide to form a 5′ Az-8mer substrate analog (Az-8mer). 5′ ^{32}P-labeled ribozyme (20 nM) was incubated at 37 °C with the Az-8mer (1 nM) and then irradiated at room temperature with UV light. The apparent K_D for binding of similar products to the ribozyme is about 3−5 nM (Perrotta and Been, unpublished data); therefore, we expect most of the Az-8mer to be bound to the matched ribozyme prior to irradiation.

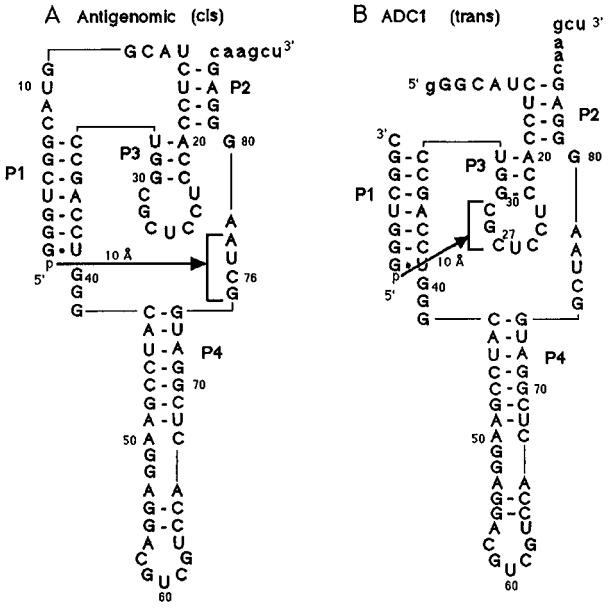

FIGURE 3: Locations of cross-links with the cleavage site phosphate. (A) Intramolecular cross-links in SA1-2P (and dSIVP). The lowercase "p" (on the left side of each panel) corresponds to the Az-containing cleavage site phosphate. Positions cross-linked to the cleavage site phosphate in 100 mM Na^+ (Na) or 10 mM Mg^{2+} (Mg) are indicated. (B) Cross-links of an 8mer substrate analog to sequences in ADC1 (and ADC3).

trans-Acting ribozymes with cross-links to the substrate analog were detected by fractionation on polyacrylamide gels containing urea. Cross-linking would give a branched molecule that should be retarded in the gel relative to the uncross-linked ribozyme. UV irradiation of ADC1 and the Az-8mer generated two closely migrating species that ran more slowly than the untreated ribozyme (Figure 4A). These products accounted for 2.9% and 2.8% of the total ribozyme (lane 6) and were not observed in the absence of UV irradiation (lane 5). Because these reactions were done with about 20-fold excess ribozyme, the maximum amount of labeled ribozyme that could be cross-linked to the substrate analog is 5%. Therefore, the amount of ADC1 cross-linked to the substrate analog suggests that this reaction may be very efficient. Two UV-dependent bands were also seen when ADC3 was incubated with Az-8mer and UV irradiated (Figure 4A, lane 18). In a control for nonspecific binding, ADC2, which has an altered specificity and will not bind substrates with the 8mer sequence (Perrotta & Been, 1992), did not produce visible slower migrating species (lane 12). Ribozymes incubated without Az-8mer (lanes 1, 2, 7, 8, 13, and 14) or with nonderivatized 8mer (lanes 3, 4, 9, 10, 15, and 16), with and without UV treatment, migrated only as the starting material. The slower migrating bands did not form when GTP-primed 8mer RNA was used in a complete set of parallel reactions (data not shown). Generation of the slower migrating bands seen with ADC1 and ADC3 (lanes 6 and 18) were thus dependent on UV light treatment and the derivatized product analog, suggesting that these bands were species resulting from cross-linking the Az-8mer to the ribozyme.

Cleavage activity of these *trans*-acting ribozymes requires either Mg^{2+} or Ca^{2+} but is not detectable in monovalent cations such as Na^+ (Puttaraju et al., 1993). Both slower migrating species were generated when Ca^{2+} was substituted for Mg^{2+}, but neither formed in Na^+ alone (data not shown).

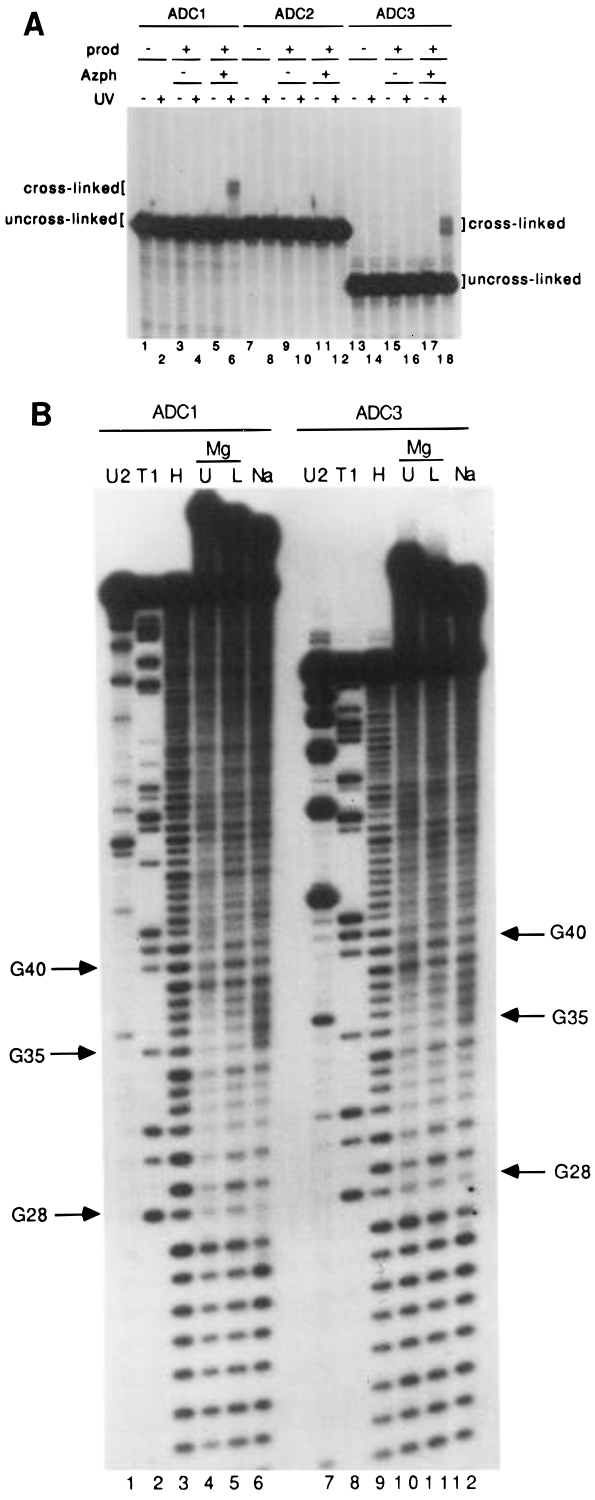

FIGURE 4: Intermolecular cross-linking. (A) Cross-linking of *trans*-acting ribozymes ADC1, ADC2, and ADC3 with 8mer analogs. The 5′ end-labeled ribozyme was UV irradiated (+UV) in the presence of GMPS-primed 8mer product analog (+prod) derivatized with azidophenacyl bromide/methanol (+Azph). Samples were analyzed as described in Figure 2A. Controls in which the UV irradiation, 8mer analog, or derivatization was omitted are also shown. The bracketed regions labeled "cross-linked" appear to be two bands that migrate very close together. (B) Mapping the positions of the cross-linked product on ADC1 and ADC3. Gel-purified cross-linked species of ADC1 (lanes 4−6) or ADC3 (lanes 10−12) generated in the presence of 10 mM Mg^{2+} (Mg, lanes 4, 5, 10, and 11) or 100 mM Na^+ (Na, lanes 6 and 12) were partially hydrolyzed with alkali and analyzed on a sequencing gel. U, upper or slower migrating band formed in Mg^{2+}; L, lower or faster migrating band formed in Mg^{2+}. Lanes 1−3 and 7−9 were sequencing markers of 5′ end-labeled ribozyme RNA.

However, in 100 mM Na^+, a single species which migrated just above the uncross-linked material was generated.

The position of the cross-link in the ribozyme was again identified by partial alkaline hydrolysis of the cross-linked species. In this case the 5′ end was labeled, and small end-labeled linear fragments released due to cleavage between the 5′ end and the cross-link should produce a uniform ladder on a sequencing gel. Fragments resulting from cleavage distal to the cross-linked positions will be shifted in the gel due to the additional eight nucleotides of the attached product analog. The cross-linked species from ADC1 and ADC3 generated in the presence of Mg^{2+} and Na^+ were isolated from a preparative gel and then partially hydrolyzed. The slower migrating band from RNA cross-linked in Mg^{2+} gave a clear ladder of fragments from the bottom of the gel to position 27 (Figure 4B, lanes 4 and 10). There was a gap in the ladder starting after nt 27 (lanes 4 and 10), suggesting extensive cross-linking to position G28. After the gap, a ladder resumed at about nt 39, but with significant background smearing (lanes 4 and 10). The lack of clarity of the hydrolysis ladder after the gap may be inherent to a Y-shaped structure or could result from these products containing a heterogeneous mixture of branched structures. A similar pattern was seen for the faster migrating of the two cross-linked species generated in Mg^{2+}(lanes 5 and 11); however, in this case, the gap in the ladder was less distinct: it resumed at about nt 37 and the gap contained a relatively intense band at C29 (lanes 5 and 11). It is very difficult to interpret the significance of the difference between the patterns generated with the two Mg^{2+} dependent cross-linked RNAs. It is possible that the difference reflects nitrene insertions into different nucleotides or different positions of the same nucleotide and that these result in altered mobility. Although we have seen no evidence for an alkaline-labile bond at the photocross-link, it is a possibility and could cause additional bands to be visible in the gap. The diffuse 9−10 nucleotide gap seen for the faster migrating of the two cross-links generated in the presence of Mg^{2+} might also be explained by some cross-linking at G28 and perhaps more at G30 and G31. For the cross-linked species generated in the presence of Na^+, the hydrolysis ladder was uniform at the bottom of the gel but decreased in intensity after nt 26 and 27 (lanes 6 and 12). After this gap, the ladder continued at about position 35 but with background smearing (lanes 6 and 12). Thus, in the presence of Na^+, the cross-links appeared to form with nucleotides C27 and G28, causing a gap of about 7−8 nucleotides in the hydrolysis ladder. Addition of Mg^{2+} appears to cause a shift in the position of L3 relative to the cleavage site; cross-links form to position G28 and perhaps also to two or more additional nucleotides on the 3′ side of L3 and P3 (C29 & G30).

All of the intermolecular cross-links were to the 3′ side of L3 and P3 (Figure 3B), which is a region not detected with the intramolecular cross-links. It was possible that the Az-8mer also cross-linked to the J4/2 region nearer the 3′ end of the ribozyme but had gone undetected due to the lack of resolution of the fragments closer to the 3′ end. To test this, the reactions were repeated using 3′ end-labeled ribozyme RNA, and positions of cross-links were identified in the single slowly migrating species. There was still a gap in the L3 and P3 region which could not be well resolved, but no gap was apparent in the J4/2 region (data not shown). We consider possible explanations for these differences in more detail in the discussion but suggest here that the two methods could be complementary and thereby identify two regions close to the cleavage site phosphate.

Fe(II)−EDTA Cleavage of the 3′ Cleavage Product of the cis-Acting Ribozymes. The structures of three different *cis* ribozyme sequences were studied in solution by using Fe(II)−EDTA to generate hydroxyl radical damage to solvent accessible regions. The 3′ cleavage products of an antigenomic RNA sequence (SA1-2; Figure 1A) (Perrotta & Been, 1991), an antigenomic RNA sequence with a shortened P4 (dSIV; Figure 1A) (Been & Perrotta, 1991), and a genomic RNA sequence (SD106; Figure 1B) (Perrotta & Been, 1990) were examined. Studying the 3′ cleavage product RNAs was justified on the grounds that, because a single nucleotide 5′ to the cleavage site is sufficient for cleavage activity (Perrotta & Been, 1990), the catalytic domain of the ribozyme must reside almost entirely 3′ to the cleavage site. The conditions used for probing the structures were chosen to be similar to conditions under which self-cleavage activity was greatest: 10 mM Mg^{2+} and 1−5 M urea at 25−42 °C and pH 7.5 (Rosenstein & Been, 1990).

dSIV 3′ product RNA (Figure 1A) was 5′ end-labeled and incubated with and without Mg^{2+} at 42 °C. This was followed by treatment with Fe(II)−EDTA at 42 °C using the molecular oxygen method (Burkhoff & Tullius, 1987). Fractionation of Fe(II)−EDTA-treated RNA resulted in a ladder of fragments (Figure 5A, lanes 3, 4, 7, and 8). In the absence of Fe(II)−EDTA, very little cleavage of the RNA occurred (lanes 1, 2, 5, and 6). In the absence of Mg^{2+}, the ladder was fairly uniform, although there were three regions where cleavage was somewhat less intense (lane 3). In the presence of Mg^{2+}, there was additional loss of band intensity in these regions (lane 4). In the presence of 1.25 M urea, protection from Fe(II)−EDTA cleavage became even more apparent (compare lane 8 with lane 4 in Figure 5A). The decreased intensity of these bands, under conditions where the ribozyme is active and the RNA folded (Rosenstein & Been, 1991), suggested that these regions of the molecule were protected from solvent (Latham & Cech, 1989).

To map the location of protection from hydroxyl radical cleavage it is necessary to take into account the nature of the cleavage products. Sequencing enzymes cut 3′ of a specific nucleotide, leaving a 3′ phosphate. Hydroxyl radical cleavage at the same nucleotide, however, results in destruction of the ribose (Tullius, 1987) and, therefore, creates fragments that are one nucleotide shorter than the sequencing products. Therefore, when starting with a 5′ end-labeled molecule and assigning positions using the comigrating fragment in the sequencing ladder, a decreased intensity of a fragment in the hydroxyl radical cleavage lane would indicate protection at the nucleotide corresponding to one immediately 3′ of that position. Protection was observed at nucleotide positions 22 and 23 in the 5′ side of P3 and L3, nucleotides 32 and 33 at the junction of P3 and P1 and nucleotides 76 and 77 in J4/2 (Figure 5A). Also protected, but to a lesser amount, were positions 27 and 40−42 (data not shown). The protected regions for the full-length antigenomic (SA1-2) RNA appeared to be essentially identical to those seen with the dSIV RNA (data not shown).

The genomic 3′ cleavage product RNA (SD106) was similarly examined, although higher concentrations of urea were used in this case to enhance the appearance of protected regions in Mg^{2+} (Figure 5B). As with the antigenomic sequence, the pattern of Fe(II)−EDTA cleavage changed when Mg^{2+} was included in the reaction. Qualitatively, the

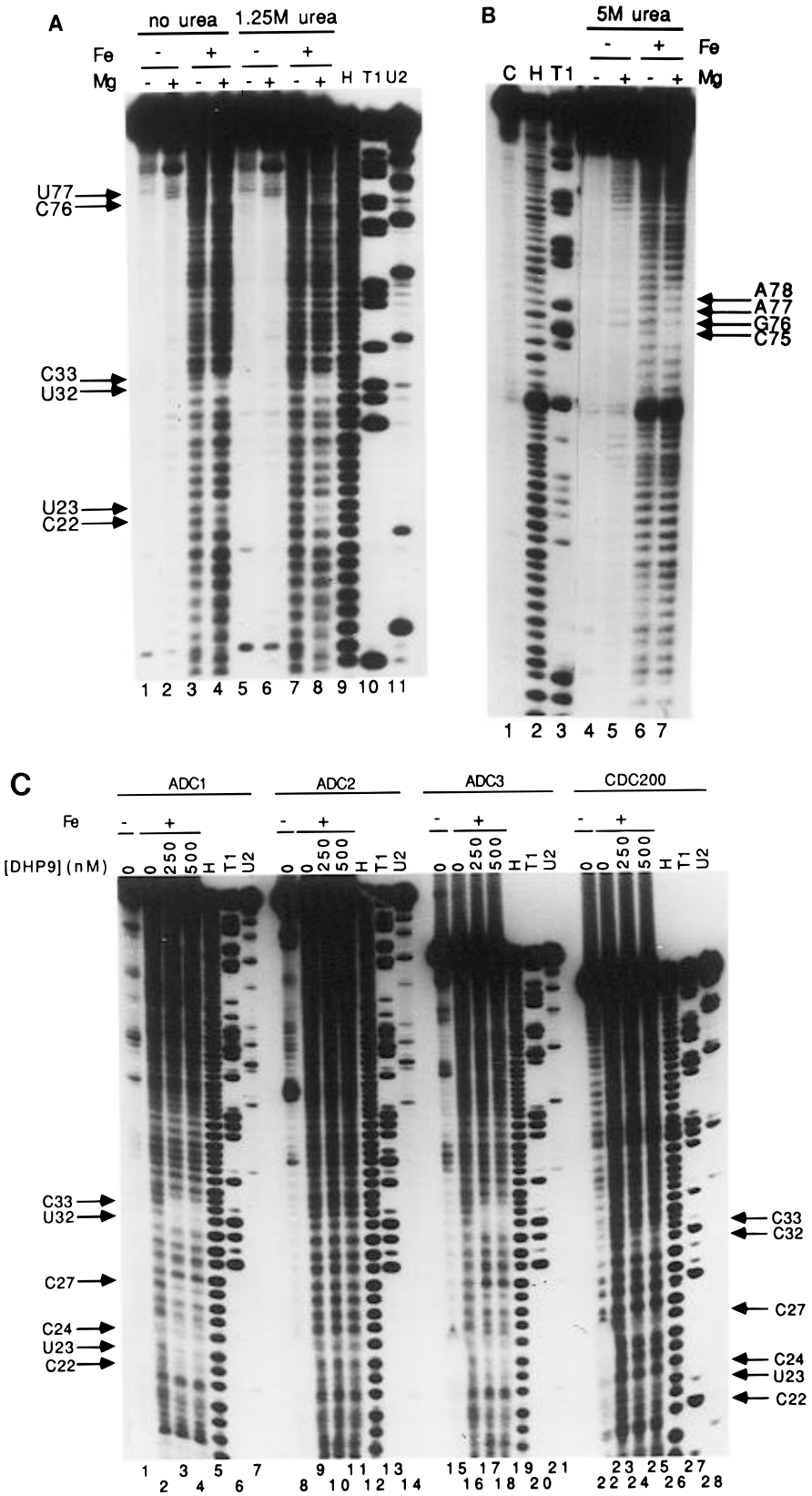

FIGURE 5: Hydroxyl radical footprinting. (A) Fe(II)−EDTA cleavage of dSIV RNA. The 5′ end-labeled 3′ self-cleavage product RNA was treated with Fe(II)−EDTA (+Fe) in the presence of Mg^{2+} (+Mg) and urea using the molecular oxygen method. The sequences that are more protected from cleavage are marked with arrows. Sequencing markers were as follows: H, alkaline hydrolysis (lane 9); T1, G ladder (lane 10); and U2, A ladder (lane 11). Controls in which either Mg^{2+} or Fe(II) were omitted are also shown. (B) Fe(II)−EDTA cleavage of SD106 genomic RNA. Reactions were performed as described in Figure 2, except the urea concentration was increased to 5 M. Sequencing lanes: C, no treatment; H, alkaline hydrolysis; T1, G ladder. (C) Protection from Fe(II)−EDTA cleavage of *trans*-acting ribozymes ADC1, ADC2, ADC3, and CDC200. The 5′ end-labeled ribozyme and 0, 250, or 500 nM unlabeled 7mer product RNA, DHP9, was reacted with Fe(II)−EDTA (+Fe) using the hydrogen peroxide method as described in Experimental Procedures.

results were similar when the urea was omitted, but there was less contrast between accessible and protected regions (data not shown). The major regions of protection in Mg^{2+} (Figure 6B) corresponded to positions 74−78 (J4/2), 19−

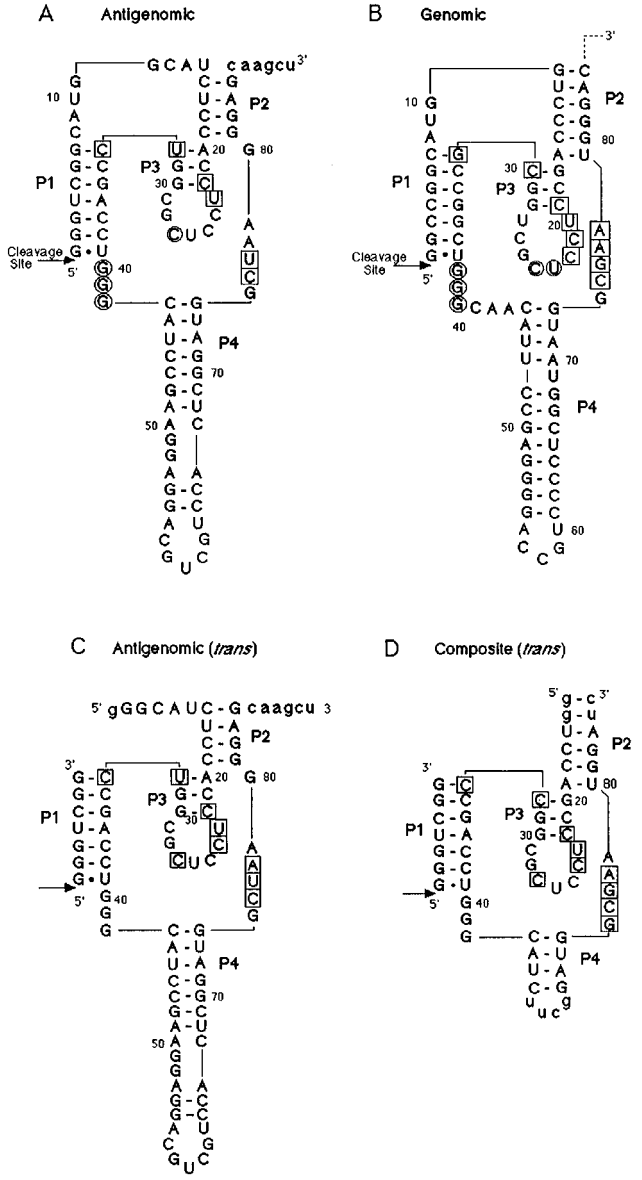

FIGURE 6: Summary of protection data. The data are compiled from results shown in Figure 5 and from other data not shown. Major sites of protection are boxed, and minor sites of protection are circled. (A) SA1-2 3′ cleavage product RNA. (B) SD106 3′ cleavage product RNA. (C) ADC1 paired with product oligonucleotide, DHP9. (D) CDC200 paired with DHP9.

22 (P3 and L3), and 30 and 31 (P3 and P1) (Figure 5B and data not shown); original films also revealed weaker protection at positions 23, 24 (L3), and 38−40 (J1/4). A summary of these results on the secondary structures reveals similar regions of protection for both ribozymes (Figure 6A and B).

Fe(II)−EDTA Cleavage Analysis of trans-Acting Ribozymes. Because the cross-linking results had raised the possibility of alternative structures for the *cis* and *trans* ribozymes, the Fe(II)−EDTA analysis was extended to several *trans*-acting HDV-derived ribozymes: ADC1, ADC2, and ADC3 (Figure 1C), as well as CDC200 (Figure 1D). CDC200 is a minimized *trans*-acting composite ribozyme-containing sequences from both the genomic and antigenomic ribozymes with the substrate specificity of ADC1 and ADC3 (Been et al., 1992).

The ribozyme RNA was 5′ end-labeled and preincubated at 37 °C in Mg^{2+}, with and without a 7mer product oligonucleotide (DHP9, 5′-GGGUCGG). This RNA was then reacted with hydroxyl radical at room temperature. In the presence of Mg^{2+} but no oligonucleotide, the ribozyme RNA was randomly cleaved to generate a uniform ladder of fragments (Figure 5C, lanes 2, 9, 16, and 23). With the oligonucleotide present in concentrations of 250 or 500 nM, there were regions in ribozymes ADC1, ADC3, and CDC200 which were protected from cleavage (lanes 3, 4, 17, 18, 24, and 25). Under these conditions, we would expect most ribozyme to contain bound product. The protected positions in ADC1 and ADC3 corresponded to nt 22 (P3), 23, 24, and 27 (L3), 32 (P3), 33 (P1), and 76−78 (J4/2) (Figure 6C); CDC200 had the same regions along with position 75 protected (Figure 6D). These protected positions were in regions of the RNA secondary structure that were also protected in the self-cleavage product of the antigenomic RNA (compare Figure 6A and B with C and D). Furthermore, these regions of protection are not due to nonspecific oligonucleotide binding because there were no protected regions in ribozyme ADC2 under the same conditions (Figure 5C, lanes 10 and 11).

DISCUSSION

We have used two dissimilar approaches to uncover consonant properties of the tertiary structure of the HDV self-cleaving RNAs. Photocross-links revealed two regions close to the cleavage site phosphate in the antigenomic RNA: the 5′ region of J4/2 and the 3′ side of L3 and P3 (Figure 3). The absence of hydroxyl radical cleavage at specific sites in both the genomic and antigenomic self-cleaving elements suggested that these RNAs fold to generate solvent-inaccessible regions in the 5′ side of P3 and L3, at the junction of P3 and P1, and in J4/2 (Figure 6). In the *cis* forms, there was also some protection of the 3G's in J1/4, but this was not seen in the *trans* form of the ribozyme. Together these data suggests a fairly compact structure that places the cleavage site phosphate in or near a relatively solvent inaccessible interior portion of the molecule.

The azidophenacyl reagent was used in much the same way it has been used previously with other ribozymes (Burgin & Pace, 1990; Nolan et al., 1993; Wang et al., 1993), except that we had to use a different method to identify cross-linked positions because of the lack of an adequate primer binding site for mapping with reverse transcriptase. The azidophenyl group is about 9 Å in length, which is less than the diameter of an A-form helix and thus proves very useful for identification of positions in the secondary structure that are very close to the active site phosphate. For the HDV ribozymes, the formation and identification of cross-linked RNAs was supported by a dependence on GMPS, the azidophenacyl moiety and UV light. We put forward three arguments that these cross-links are representative of the major RNA conformation and are reflective of the active species. First, in SA1-2P RNA and the smaller dSIVP RNA, the locations of the cross-links were the same. Likewise for the *trans*-acting RNA, the Az-substrate analog cross-linked to both ribozyme ADC1 and ADC3 in identical locations, whereas ADC2, the ribozyme with altered substrate specificity, did not form cross-links with the same analog. Second, conditions that altered the location of the cross-link paralleled the effect of those conditions on activity. Rapid self-cleavage of HDV RNA requires divalent cations such as Mg^{2+} or Ca^{2+} (Wu et al., 1989). A shift in position of the cross-link by 1−2 nucleotides occurred in the absence of Mg^{2+} or when 100 mM Na^{+} was substituted for the divalent cation. This result agrees with ribonuclease probing

data which showed that the details of the cutting patterns in Mg^{2+} could not be duplicated in the presence of up to 1 M Na^{+} alone (S.P.R., unpublished data). Finally, the positions of the cross-links from the cleavage site phosphate to the 3′ side of L3 (G28 and perhaps others) and J4/2 (G75, C76) in the antigenomic RNA are consistent with conserved and functionally important sequences in both the antigenomic and genomic HDV ribozymes.

There appear to be three possible explanations for the finding that cross-links formed to different regions in the intermolecular (*trans*) versus intramolecular (*cis*) forms of the ribozyme. First, the structure of the intermolecular form of the ribozyme may be significantly different from the intramolecular form. This would appear to be unlikely because of the similarity of all the cleavage patterns obtained with Fe(II)−EDTA. Second, due to subtle differences in the folding or assembly of the two forms, or in the flexibility of P1, the azidophenacyl group may be in a slightly different position so that one region or the other is favored for cross-link formation. Third, the detection and purification of the cross-linked forms by gel mobility shift enriches for a different subset of cross-linked species in each case. If either one of the latter two possibilities is correct, then both regions may be near the cleavage site phosphate, suggesting that the cleavage site is surrounded by a pocket formed by L3 and part of J4/2. A recent paper by Bravo et al. (1996) provides data consistent with this interpretation. There, deoxy 4-thiouracil was used as the photoaffinity reagent at the 5′ end of a substrate analog bound to a ribozyme essentially identical to ADC1. Their results, similar to ours, were that L3 and J4/2 are close to the cleavage site. One difference in the findings was that they found cross-links more in the 5′ side of L3. The interpretation of these differences will depend on how L3 is modeled, but together the approaches suggest a very intimate relationship between the end of P1 and L3 and gave very similar overall pictures of the tertiary folding of the antigenomic sequence.

A metal ion-dependent change in the structure was seen in both sets of cross-linking experiments. Both monovalent or divalent ions are known to stabilize RNA structure (Jack et al., 1977), but divalent metal ions may have additional specific roles in the structure and activity of catalytic RNA (Chowrira et al., 1993; Christian & Yarus, 1993; Dahm & Uhlenbeck, 1991; Grosshans & Cech, 1989; Perreault & Altman, 1993; Piccirilli et al., 1993; Pyle, 1993; Smith & Pace, 1993; Steitz & Steitz, 1993). Finding that divalent cations changed the position or nature of the cross-links suggests that Mg^{2+} ion coordination to unknown ligands causes a conformational change. This change brings specific nucleotides in L3 and J4/2 in closer proximity to the cleavage site, perhaps as specifically positioned components of the active site. In addition to the expected structural changes due to binding of Mg^{2+} to the RNA backbone, it is possible that specific binding of Mg^{2+} to the cleavage site phosphate would have a direct effect on the orientation of the azidophenyl group.

The Fe(II)−EDTA cleavage results provide evidence that the sequences are folding into compact structures in solution. There was good agreement between the conditions that gave optimal activity (Rosenstein & Been, 1990) and conditions that gave the clearest hydroxyl radical protection. Thus, it seems likely that the Fe(II)−EDTA data were obtained on properly folded molecules because both Mg^{2+} and denaturant intensified the protection from hydroxyl radical cleavage. It was also persuasive that the protected regions were mapped to almost identical regions of the genomic and antigenomic secondary structures. This was the case for both the full-length genomic and antigenomic sequences and the antigenomic sequence with a shortened stem IV. Although it is remotely possible that these molecules all misfold into similar incorrect structures, it is much more likely that the similar data sets would result from correctly folded structures. The results with the *trans*-acting RNA also gives confidence that the data from Fe(II)−EDTA cleavage were obtained from catalytically relevant structures. Protection from hydroxyl radical for the *trans*-acting ribozymes was dependent on the presence of substrate analog and occurred in the same regions as those for the *cis*-acting RNAs; this was true for both the antigenomic derived ribozymes (ADC1 and ADC3) and for the composite (CDC200) ribozyme. This suggested that the *trans*-acting ribozymes, when bound to product, were adopting the same structures seen with the *cis*-acting ribozymes. The lack of protection of ribozymes in the free form suggests that there is either little preformed structure or insufficient structure to generate solvent-inaccessible sites. The ribozyme ADC2 with altered substrate specificity showed no regions of protection with or without product, again suggesting that it is unlikely that the protected sequences seen for the matched ribozymes could be due to nonspecific product binding.

Fe(II)−EDTA has also been to probe the structures of group I introns (Latham & Cech, 1989; Heuer et al., 1991). Latham and Cech (1989) had shown that the technique worked very well on tRNA (an RNA about the size of the HDV ribozyme), and there was good agreement between the tRNA protection data and the crystal structure. For the HDV genomic and antigenomic RNAs, protected regions correspond to positions already identified by mutagenesis (Kumar et al., 1992; Perrotta & Been, 1996; Tanner & Cech, 1987; Wu & Huang, 1992), chemical modification (Kumar et al., 1994), and modification interference (Belinsky et al., 1993) to be important. The location of the cleavage site phosphate in or near these solvent protected regions also supports the idea that these nucleotides may have important roles in the catalytic activity of the RNA. Therefore, it appears that the HDV ribozymes form a compact structure with a specified inside and outside.

The Fe(II)−EDTA cleavage data may also reveal a specific feature of the ribozyme structure. Protection was seen at two nucleotides which reside at the junction P3 and P1. When the current secondary structures were proposed, it was noted that because P3 is continuous in the 3′ strand with P1 and in the 5′ strand with P2, P3 could potentially stack on either P1 or P2 (Rosenstein & Been, 1990). The cross-linking data, which places L3 close to the cleavage site would appear to rule out the P1−P3 stacking interaction and will require a sharp bend in the strand forming the 3′ side of P1 and P3. Also, data indicate that sequence in P3 (Been et al., 1992; Thill et al., 1993) and L3 (Perrotta & Been, 1996; Thill et al., 1993) is important for cleavage. This strict requirement would appear to be inconsistent with a P1−P3 stacking interaction as that would distance both elements from the cleavage site. Protection from cleavage at the P1/P3 junction is perhaps further evidence for a sharp bend between P1 and P3. In the model of the genomic ribozyme structure proposed by Tanner et al. (1994), P3 is bent at a sharp angle relative to P1 and these two nucleotides (C30 and G31) are buried along with the strongly protected regions of L3. On

the other hand, the protected sequences in J4/2 and regions of minor protection in J1/4 would appear to be very accessible in that model.

The model proposed by Tanner et al. (1995) is a fair and useful representation of what is currently known about these ribozymes. Data from this and previous work suggest the following picture. The ribozymes contain four paired sequences (P1−P4) which are presumably A-form helices and define three single-stranded joining sequences (J1/2, J1/4, and J4/2) and two loops (L3 and L4). The helices are thought to serve mainly a structural function although P1 contains the cleavage site and P3 displays some sequence requirements (Been et al., 1992; Thill et al., 1993). Of the single-stranded regions, L3, J1/4, and J4/2 contain sequences essential for catalytic activity. The cleavage site, located at the 5′ end of P1, we now know is within 9−10 Å of the 5′ portion of J4/2 and the 3′ side of L3. This would suggest that the 5′ end of P1 is either sandwiched between L3 and J4/2 or fits into a cleft or pocket formed by these structures. In addition, J1/4, which is continuous with the 3′ side of P1 and contains conserved bases essential for activity (Perrotta & Been, 1996; Tanner et al., 1994), would have to be close to the cleavage site. A binding pocket composed of essential nucleotides in L3, J1/4, and J4/2 would be consistent with most of the site-specific mutagenesis and chemical modification data available for the HDV ribozymes (Belinsky et al., 1993; Kumar et al., 1993, Kumar et al., 1994; Perrotta & Been, 1996; Tanner et al., 1994; Thill et al., 1993; Wu & Huang, 1992; Wu et al., 1993).

ACKNOWLEDGMENT

We thank A. Perrotta, T. Wadkins, and G. Wickham for comments on the manuscript.

REFERENCES

Been, M. D. (1994) *Trends Biochem. Sci. 19*, 251−256.
Been, M. D., & Perrotta, A. T. (1991) *Science 252*, 434−437.
Been, M. D., & Perrotta, A. T. (1995) *RNA 1*, 1061−1070.
Been, M. D., Perrotta, A. T., & Rosenstein, S. P. (1992) *Biochemistry 31*, 11843−11852.
Belinsky, M. G., Britton, E., & Dinter-Gottlieb, G. (1993) *FASEB J. 7*, 130−136.
Branch, A. D., & Robertson, H. D. (1991) *Proc. Natl. Acad. Sci. U.S.A. 88*, 10163−10167.
Bravo, C., Lescure, F., Laugâa, P., Fourrey, J.-L., & Favre, A. (1996) *Nucleic Acids Res. 24*, 1351−1360.
Burgin, A. B., & Pace, N. R. (1990) *EMBO J. 9*, 4111−4118.
Burkhoff, A. M., & Tullius, T. D. (1987) *Cell 48*, 935−943.
Celander, D. W., & Cech, T. R. (1990) *Biochemistry 29*, 1355−1361.
Chowrira, B. M., Berzal-Herranz, A., & Burke, J. M. (1993) *Biochemistry 32*, 1088−1095.
Christian, E. L., & Yarus, M. (1993) *Biochemistry 32*, 4475−4480.
Dahm, S. C., & Uhlenbeck, O. C. (1991) *Biochemistry 30*, 9464−9469.
Davanloo, P., Rosenberg, A. H., Dunn, J. J., & Studier, F. W. (1984) *Proc. Natl. Acad. Sci. U.S.A. 81*, 2035−2039.
Grosshans, C. A., & Cech, T. R. (1989) *Biochemistry 28*, 6888−6894.
Hertzberg, R. P., & Dervan, P. B. (1984) *Biochemistry 23*, 3934−3945.
Heuer, T. S., Chandry, P. S., Belfort, M., Celander, D. W., & Cech, T. R. (1991) *Proc. Natl. Acad. Sci. U.S.A. 88*, 11105−11109.
Jack, A., Ladner, J. E., Rhodes, D., Brown, R. S., & Klug, A. (1977) *J. Mol. Biol. 111*, 315−328.
Jeng, K.-S., Daniel, A., & Lai, M. M. C. (1996) *J. Virol. 70*, 2403−2410.
Kumar, P. K. R., Suh, Y.-A., Miyashiro, H., Nishikawa, F., Kawakami, J., Taira, K., & Nishikawa, S. (1992) *Nucleic Acids Res. 20*, 3919−3924.
Kumar, P. K. R., Suh, Y.-A., Taira, K., & Nishikawa, S. (1993) *FASEB J. 7*, 124−129.
Kumar, P. K. R., Taira, K., & Nishikawa, S. (1994) *Biochemistry 33*, 583−592.
Kuo, M. Y.-P., Sharmeen, L., Dinter-Gottleib, G., & Taylor, J. (1988) *J. Virol. 62*, 4439−4444.
Latham, J. A., & Cech, T. R. (1989) *Science 245*, 276−282.
MacNaughton, T. B., Wang, Y.-J., & Lai, M. M. C. (1993) *J. Virol. 67*, 2228−2234.
Maniatis, T., Fritsch, E. F., & Sambrook, J. (1982) *Molecular Cloning: A Laboratory Manual*, Cold Spring Harbor Laboratory, Cold Spring Harbor, NY.
Nolan, J. M., Burke, D. H., & Pace, N. R. (1993) *Science 261*, 762−765.
Perreault, J.-P., & Altman, S. (1993) *J. Mol. Biol. 230*, 750−756.
Perrotta, A. T., & Been, M. D. (1990) *Nucleic Acids Res. 18*, 6821−6827.
Perrotta, A. T., & Been, M. D. (1991) *Nature 350*, 434−436.
Perrotta, A. T., & Been, M. D. (1992) *Biochemistry 31*, 16−21.
Perrotta, A. T., & Been, M. D. (1993) *Nucleic Acids Res. 21*, 3959−3965.
Perrotta, A. T., & Been, M. D. (1996) *Nucleic Acids Res. 24*, 1314−1321.
Piccirilli, J. A., Vyle, J. S., Caruthers, M. H., & Cech, T. R. (1993) *Nature 361*, 85−88.
Puttaraju, M., Perrotta, A., & Been, M. (1993) *Nucleic Acids Res. 21*, 4253−4258.
Pyle, A. M. (1993) *Science 261*, 709−714.
Rosenstein, S. P., & Been, M. D. (1990) *Biochemistry 29*, 8011−8016.
Rosenstein, S. P., & Been, M. D. (1991) *Nucleic Acids Res. 19*, 5409−5416.
Sharmeen, L., Kuo, M. Y.-P., Dinter-Gottlieb, G., & Taylor, J. (1988) *J. Virol. 62*, 2674−2679.
Smith, D., & Pace, N. R. (1993) *Biochemistry 32*, 5273−5281.
Steitz, T. A., & Steitz, J. A. (1993) *Proc. Natl. Acad. Sci. U.S.A. 90*, 6498−6502.
Tanner, N. K., & Cech, T. R. (1987) *Biochemistry 26*, 3330−3340.
Tanner, N. K., Schaff, S., Thill, G., Petit-Koskas, E., Crain-Denoyelle, A.-M., & Westhof, E. (1994) *Curr. Biol. 4*, 488−497.
Thill, G., Vasseur, M., & Tanner, N. K. (1993) *Biochemistry 32*, 4254−4262.
Tullius, T. D. (1987) *Trends Biochem. Sci. 12*, 297−300.
Wang, J.-F., Downs, W. D., & Cech, T. R. (1993) *Science 260*, 504−508.
Wu, H.-N., & Huang, Z.-S. (1992) *Nucleic Acids Res. 20*, 5937−5941.
Wu, H.-N., Lin, Y.-J., Lin, F.-P., Makino, S., Chang, M.-F., & Lai, M. M. C. (1989) *Proc. Natl. Acad. Sci. U.S.A. 86*, 1831−1835.
Wu, H.-N., Wang, Y.-J., Hung, C.-F., Lee, H.-J., & Lai, M. M. C. (1992) *J. Mol. Biol. 223*, 233−245.
Wu, H.-N., Lee, J.-Y., Huang, H.-W., Huang, Y.-s., & Hsueh, T.-G. (1993) *Nucleic Acids Res. 21*, 4193−4199.

BI9609984